Int. J. Heat Mass Transfer. Vol. 7, pp. 539–548 Pergamon Press 1964. Printed in Great Britain

HIGH FLUX SOLID–LIQUID MASS TRANSFER

ALAN S. EMANUEL†
Department of Chemical Engineering, University of California, Berkeley, California

and

DONALD R. OLANDER
Inorganic Materials Research Division of the Lawrence Radiation Laboratory and the Department of Nuclear Engineering, University of California, Berkeley, California

(*Received* 14 *December* 1962; *and in revised form* 4 *November* 1963)

Abstract—The effect of large concentration gradients upon the rate of mass transfer from a rotating disc has been measured experimentally and compared with theory. Measured rates were found to agree with the numerical solutions of the variable property, finite interfacial velocity diffusion equation. The data were also compared with approximate perturbation and integral solutions of the diffusion equation. The systems investigated were benzoic acid, potassium bromide, sucrose, and copper sulfate in water. Variations in density, viscosity and diffusivity and the existence of a diffusion-induced interfacial velocity can result in differences between the constant property, zero interfacial velocity and the actual Sherwood numbers as large as a factor of two.

NOMENCLATURE

D, diffusion coefficient [cm²/s];
k_w, mass-transfer coefficient based upon mass fraction driving force, defined by equation (5) [cm/s];
n, solute mass flux relative to a stationary observer [g/cm² s];
S, ratio of solvent to solute mass fluxes at the surface;
Sc, Schmidt number;
Sh, Sherwood number, defined by equation (6);
W, solute mass fraction;
y, distance normal to the disc;
z, film thickness.

Greek symbols

α, coefficient of first term of power series expansion of dimensionless axial velocity about $\eta = 0$;
η, dimensionless axial distance $y(\omega/\nu_o)^{1/2}$;
θ, dimensionless concentration $(W - W_\infty)/(W_o - W_\infty)$;
ϵ_V, interfacial velocity parameter, equation (3);
ϵ_D, diffusivity variation parameter, equation (9);
ϵ_ρ, density variation parameter, equation (4);
ρ, solution density [g/cm³];
μ, solution viscosity [P];
ν, kinematic viscosity [cm²/s];
ω, rotational speed of disc [s⁻¹];
β, γ, constants describing diffusivity variations, equation (10);
δ, dimensionless diffusion boundary layer thickness (the value of η at which $\theta = 0{\cdot}01$).

Subscripts

o, at the disc surface, $\eta = 0$;
∞, in the bulk liquid, $\eta = \infty$;
lm, log-mean, $x_{lm} = (x_o - x_\infty)/\ln(x_o/x_\infty)$.

Superscripts

$*$, for constant properties and zero interfacial velocity (no mass transfer);
$'$, denotes differentiation with respect to η.

IN RECENT years, considerable attention has been given to predicting mass-transfer rates in laminar boundary-layer flows. Most of these

† Present address: Atomics Internation Division, North American Aviation, Inc., Canoga Park, California.

studies have been restricted to systems in which some or all of the properties were assumed constant. However, the physical properties of many liquid systems are strongly dependent on composition, and the variation of density, diffusivity, and viscosity across the diffusion boundary layer can have a significant effect on the mass-transfer rate. In addition, the transferring solute leaves or enters the solid surface with a finite velocity, which distorts the no mass-transfer velocity profiles and consequently alters the convective term in the diffusion equation. All of these effects become increasingly important for transfer under large concentration driving forces.

The paper describes an experimental study of the phenomena associated with high gradient transfer. The results are compared with the various approximate solutions to the diffusion equation.

The rotating disc was selected for the experimental work, since in the region of high Schmidt numbers, the mass-transfer behavior of this system is similar to that for other boundary layer-type flows (e.g. flat plate, falling liquid film). Considerable theoretical [1–4] and experimental [5, 6] background on the rotating disc system is available.

THEORY

It has been shown previously [3] that the form of the diffusion equation applicable to high Schmidt number, variable property boundary layer type flow is:

$$\theta'' + \left(\frac{D_o}{D}\right)[\alpha\, Sc_o\, \eta^2 + \epsilon_V\, \theta_o']\,\theta' - \left[\epsilon_\rho - \frac{\mathrm{d}\ln(D/D_o)}{\mathrm{d}\theta}\right](\theta')^2 = 0 \qquad (1)$$

with boundary conditions:

$$\theta(0) = 1$$

$$\theta(\infty) = 0$$

This relation is equivalent to equation (23) of reference [3] except that the term $\mathrm{d}\ln(D/D_o)/\mathrm{d}\theta$ in equation (1) above is no longer assumed to be a constant ($-\epsilon_D$), and the $L(\eta)$ term in the earlier form is neglected compared to unit (as was also done subsequently in reference 3). The retention of an arbitrary diffusivity–composition relation in the present formulation permits application of equation (1) to a wider class of binary solutions than was possible in the earlier work.

Following the notation of reference 3, the symbols in equation (1) are:

$$\alpha = \alpha^* \left(\frac{\rho_\infty\, \mu_\infty}{\rho_o\, \mu_o}\right)^{1/2} \qquad (2)$$

$$\epsilon_V = \frac{W_o - W_\infty}{1/(1+S) - W_o} \qquad (3)$$

$$\epsilon_\rho = -(W_o - W_\infty)\frac{\mathrm{d}\ln\rho}{\mathrm{d}W} = -\frac{\mathrm{d}\ln\rho}{\mathrm{d}\theta} = \text{constant}. \qquad (4)$$

Equation (2) represents Schuh's [7] method of accounting for velocity profile distortion due to viscosity changes. The parameter α^* is the sole reflection of the flow geometry in the diffusion equation; for a rotating disc, it has a value of 0·510. The parameter ϵ_V represents the effect of the diffusion-induced interfacial velocity. The parameter S in (3) is the ratio of the solvent to solute mass fluxes at the interface. In the experimental work of this study, it enters in the dissolution of $CuSO_4 \cdot 5H_2O$ to water. There is a flux of water of hydration associated with that of the copper sulfate, and S is the ratio of the two. The parameter in equation (4) is not truly a constant, but for most binary solutions, over the concentration ranges usually encountered, variation is to slight that it may be considered a constant.

A mass-transfer coefficient is defined on a mass-fraction driving force basis by

$$k_w \equiv \frac{n_o}{\rho_o\,(W_o - W_\infty)}. \qquad (5)$$

The Sherwood number is given by

$$Sh \equiv \frac{[1 - W_o(1+S)]\,k_w\,(\nu_o/\omega)^{1/2}}{D_o} = -\theta_o'. \qquad (6)$$

The middle expression in equation (6) is measurable; for comparison with theory, the

right-hand member is calculable from a solution to equation (1).

For low driving forces ($a = a^*$, $\epsilon_V = \epsilon_\rho = 0$, $D = D_o$). Sparrow and Gregg [4a] have obtained an analytical solution to equation (1):

$$Sh^* = 0{\cdot}62\,Sc_o^{1/3}. \quad (7)$$

The exact solution to the constant property, zero interfacial velocity diffusion equation using a seven-term polynomial for the axial velocity profile [equations (1) and (7) are based upon a one term approximation] shows that equation (7) is approached asymptotically as $Sc \to \infty$. At $Sc = 1000$, the constant in equation (7) is 0·60 rather than 0·62. In the presence of property variations, an exact solution to equation (1) is possible only by numerical integration; a computer program has been written for this purpose.

From a practical standpoint, an approximate analytical solution would be preferable. The perturbation technique employed previously [3] predicts:

$$\begin{aligned} Sh/Sh^* = \{&1 + 1/2\,\epsilon_\rho + 0{\cdot}262\,\epsilon_D - 0{\cdot}566\,\epsilon_V \\ &+ 1/6\,\epsilon_\rho^2 + 0{\cdot}046\,\epsilon_D^2 + 0{\cdot}407\,\epsilon_V^2 \\ &+ 0{\cdot}215\,\epsilon_\rho\,\epsilon_D - 0{\cdot}566\,\epsilon_\rho\,\epsilon_D \\ &- 0{\cdot}232\,\epsilon_D\,\epsilon_\rho\}\left(\frac{\rho_\infty \mu_\infty}{\rho_o \mu_o}\right)^{1/6}. \end{aligned} \quad (8)$$

The diffusivity variation is embodied in the parameter ϵ_D, which is:

$$\epsilon_D = -(W_o - W_\infty)\frac{\mathrm{d}\ln(D/D_o)}{\mathrm{d}W} = -\frac{\mathrm{d}\ln(D/D_o)}{\mathrm{d}\theta} = \text{constant}. \quad (9)$$

This formulation, however, is quite restricted in the range of interfacial velocities and diffusivity variations over which it can be applied. A more accurate fit to common diffusivity–composition curves can be written as a two-parameter polynomial:

$$D/D_o = 1 - \beta(1 - \theta) - \gamma(1 - \theta^2). \quad (10)$$

This relation is designed to provide accurate diffusion coefficients in the region close to the wall, where molecular diffusion predominates. It can accommodate diffusivity curves with minima, while equation (9) cannot.

A modified integral technique has been employed to obtain a solution to equation (1) using diffusivities expressed by equation (10). This result is a Sherwood number ratio given by (see Appendix):

$$\frac{Sh}{Sh^*} = \frac{(1 - 0{\cdot}222\,\gamma - 0{\cdot}167\,\beta)^2}{1 - 0{\cdot}027\,\gamma + \epsilon_V(0{\cdot}544 + 0{\cdot}012\,\gamma) - \epsilon_\rho(0{\cdot}656 - 0{\cdot}545\,\gamma - 0{\cdot}388\,\beta)}\left(\frac{\rho_\infty \mu_\infty}{\rho_o \mu_o}\right)^{1/6}. \quad (11)$$

This relation has been compared to exact numerical solution of equation (1) for 20 typical high driving force liquid systems. Over the ranges: $-0{\cdot}7 \leqslant \epsilon_V \leqslant 3{\cdot}0$, $-0{\cdot}4 \leqslant \epsilon_\rho \leqslant 0{\cdot}3$, and $0{\cdot}33 \leqslant D_\infty/D_o \leqslant 3{\cdot}0$, the integral and exact solutions of equation (10) agree to within 10 per cent. By comparison, the perturbation solution, equation (8), is much less satisfactory when $|\epsilon_V| \geqslant 0{\cdot}4$, and when the diffusivity is not an exponential function of mass fraction over the concentration interval considered.

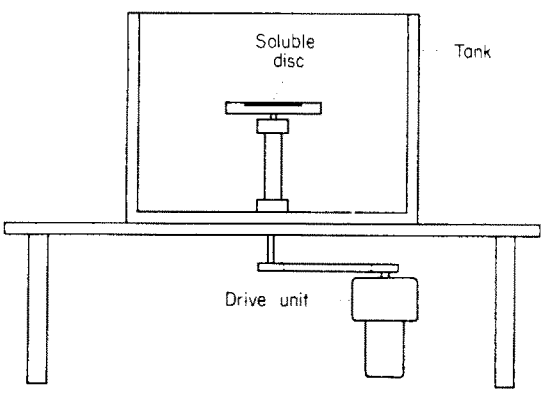

FIG. 1. Rotating disc apparatus.

EXPERIMENT

The apparatus shown in Fig. 1 was designed to measure the rate of dissolution of solid, soluble discs rotating in a quiescent liquid. Two tank sizes were used: 2 ft × 2 ft × 2 ft and 8 in × 8 in × 9 in. The tanks could be filled either with pure water or, to alter the driving force, with solutions of the disc material. All measurements were carried out at 25°C.

Four systems were studied. The solutes were benzoic acid, copper sulfate, sucrose, potassium

Table 1. Physical properties of solute–water systems at 25°C.

Solute	W_o[a]	$D_o \times 10^5$	Sc_o	$\mu_o \times 10^2$	ρ_o	$D\,(W=0) \times 10^5$	References
Benzoic acid	0·00337	0·94	946	0·89	0·997	0·94	[9]
Potassium bromide	0·404	2·55	270	0·950	1·380	2·02	[10, 11]
Copper sulfate	0·184	0·383	5800	2·23	1·210	0·85	[10, 12]
Sucrose	0·679	0·35[b]	$4·01 \times 10^5$	191·0	1·341	0·52[b]	[10]

water: $\rho = 0·997$ g/cm³; $\mu = 0·00897$ *P*.

a. saturation at 25°C; data taken from references 9 and 10.

b diffusivities for $0 \leqslant W \leqslant 0·55$ from references 13 and 14. A single value was determined from a diaphragm cell measurement at $W \approx 0·61$. All data were then combined in a single curve and extrapolated to saturation.

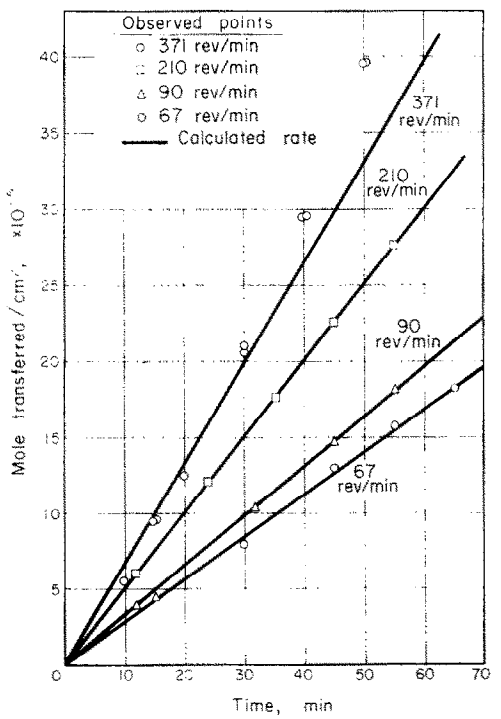

FIG. 2. Mass-transfer measurement for benzoic acid in water, 25°C. Theoretical ratio from equations (5), (6), and (7), with the constant 0·62 in equation (7) replaced by 0·60. Disc diameters of 2 and 4 in.

bromide and, in each case, the solvent was water. Benzoic acid and copper sulfate discs were formed by compacting the powdered material into smooth, solid cakes. Both 4 and 2 in dia. benzoic acid discs were used; the copper sulfate discs were of 2 in dia. The sucrose discs were formed by casting the molten material into 2 in dia. cylindrical molds which could then be attached to the rotating shaft. Disc-shaped, 1 in dia. optical crystals of potassium bromide were obtained from the Harshaw Chemical Co. Benzoic acid dissolution was measured at several different rotational speeds, while the other systems were all run at 67 rev/min.

The rate of mass transfer into pure water was determined by periodically sampling the bulk and analysing the samples for solute concentration. For transfer into solutions of finite concentration, the rate was measured by weighing the disc before and after a run. It was not possible to measure the transfer rate of copper sulfate for bulk concentrations other than zero. The compressed cake tended to absorb water, and any method which removed the absorbed water also removed an undeterminable amount of water of hydration. Additional details can be found in reference 8. The physical property of the four solute–water systems are listed in Table 1.

RESULTS AND DISCUSSION

Benzoic acid

Figure 2 presents the mass-transfer results for benzoic acid into water. This system represents nothing more than a test of the constant property, zero interfacial velocity mass-transfer behavior

of the disc system, since the solubility of benzoic acid in water is too low for any of the effects associated with large driving forces to appear. The theoretical transfer rate is based upon the seven-term velocity profile. At the Schmidt number characteristic of this system, the one-term approximation to the axial velocity gives a Sherwood number ~3 per cent too large. The good agreement between the theoretical and experimental results indicate that the hydrodynamic model based upon an infinite disc rotating in an infinite body of quiescent fluid is in fact realized in the apparatus.

At 371 rev/min, the deviation between experimental and theoretical results is appreciable. This is attributed to the tendency of the edges of the benzoic acid cake to flake off under the action of the centrifugal forces. The experimental transfer rates for the 2 and 4 in discs gave the same close agreement with the theoretical rate.

Potassium bromide

Figures 3(a) and 3(b) present the rates of transfer of KBr discs to bulk solutions of 0, 0·1, 0·25 and 0·36 mass fraction. The solid lines in the figure were calculated from the numerical solution to equation (1). In all cases, the rates computed from equation (1) were within the experimental error of the measurement. Figure 4 shows the ratios of the actual Sherwood number to that for constant properties, zero interfacial velocity (zero driving force) as a function of the driving force.† The most important high driving force effects in this system are the density variation and the interfacial velocity. The viscosity and diffusivity variations are quite small. Figure 4 shows the close agreement between the experimental points and the numerical and integral solutions to equation (1). Because of the large interfacial velocities at high driving forces, the perturbation solution is in error by as much as 15 per cent. As the driving force decreases to zero, the experimental Sherwood number ratios approach unity.

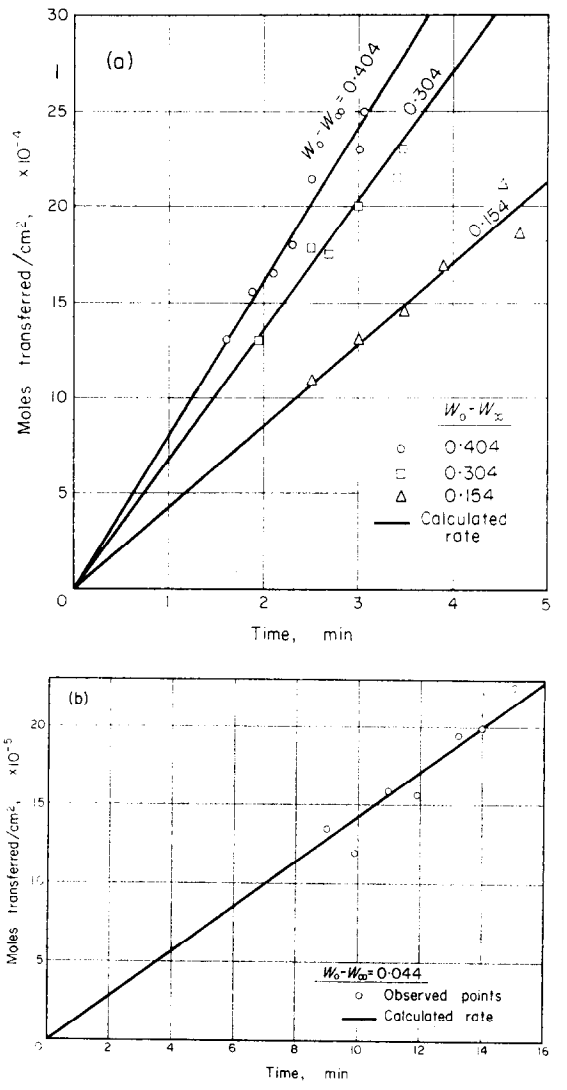

FIG. 3. Mass-transfer measurement for potassium bromide in water 25°C, 67 rev/min. Theoretical rates from equations (5), (6), and numerical solutions of equation (1). Disc diameter = 1 in.

† For the experimental Sherwood number ratios, Sh^* is calculated with the seven-term axial velocity polynomial. For the theoretical ratios, Sh^* is calculated from equation (7) since the one term axial velocity profile has also been assumed for equation (1). At $Sc = 270$ (the value for saturated KBr in water), equation (7) gives results which are 5 per cent too high. Since the numerical solution of equation (1) should also be in error by approximately this amount, the calculated ratio should be correct. However, the theoretical rates of Fig. 3 are based upon equation (1), and the actual slopes should be approximately 5 per cent smaller than those shown. This discrepancy is roughly equal to the experimental error. For the other systems, however, the Schmidt numbers are sufficiently large such that any discrepancy caused by the use of a one-term velocity profile is considerably smaller than the experimental error.

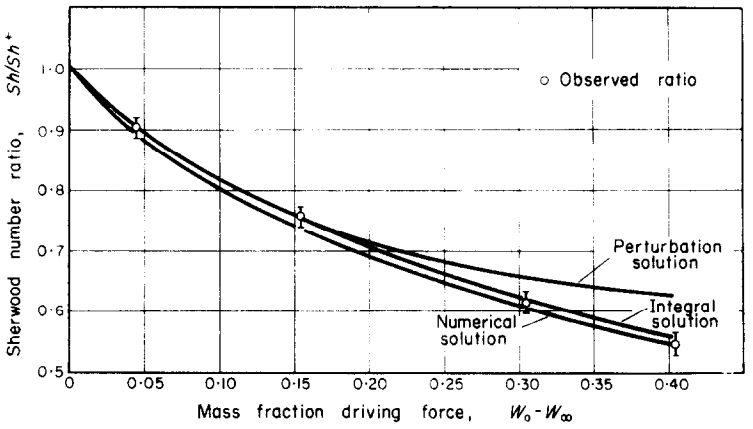

FIG. 4. Sherwood number ratio for potassium bromide.

Copper sulfate pentahydrate

This system exhibits all four of the effects associated with high driving force transfer: the diffusivity and viscosity vary by a factor of two from saturation to infinite dilution, and the density changes by 20 per cent. Because of the water of crystallization present in the disc, a solvent flux exists at the surface. The ratio of solvent-to-solute mass fluxes at the interface is equal to the weight ratio of water of hydration to $CuSO_4$ in the solid, or 0·565. The results for the saturation to infinite dilution driving force are shown in Fig. 5. Because of experimental difficulties, measurement with the bulk liquid pre-loaded with solute could not be performed. Calculated rates [based upon numerical solution of equation (1)] are plotted for $S = 0{\cdot}565$ and $S = 0$, the latter neglecting the fact that water of crystallization is present. While the difference between the slopes of the two lines is only ~5 per cent, the rate computed with $S = 0{\cdot}565$ is in better agreement with the data than that for $S = 0$. While this does not conclusively demonstrate the importance of solvent interfacial flux, the correction is clearly in the right direction.

Sucrose

This system exhibits large variations in density and diffusivity, but the most interesting feature is the viscosity, which decreases by a factor of 200 from saturation to infinite dilution. Transfer rates computed by numerical solutions of equation (1) show marked deviation from the experimental points for driving forces $> \sim 0{\cdot}1$, therefore, the lines in Fig. 6 represent best fits to the data.

At $W_0 - W_\infty = 0{\cdot}1$, the viscosity ratio (disc-to-bulk) is 10. Beyond this driving force, the major cause of the decrease in Sh/Sh^* is the viscosity change across the diffusion boundary layer. Up to $W_0 - W_\infty \sim 0{\cdot}1$, Fig. 7 indicates that the numerical and integral solutions are in good agreement with the data; beyond this, the deviations are significantly greater than the experimental precision. This discrepancy is attributed to a breakdown of the Schuh viscosity correction to the velocity profile (equation (2) and reference 7) for $\mu_0/\mu_\infty > 10$.

A more exact solution of the diffusion equation was carried out in order to account for large changes in viscosity. Briefly, this involved first solving equation (1) numerically for a particular driving force to obtain a first approximation to the concentration profile; from this, the viscosity was determined as a function of η. With this viscosity function, a more accurate expression for the dimensionless velocity profile could be derived from equations (52) and (54) of reference [3], and the diffusion equation was resolved with this new velocity expression. After three interations, the process converged to give a constant value of the Sherwood number. This value of the Sherwood number now represents the complete solution to equation (1), accounting for density and diffusivity variation and interfacial velocity, as well as for the variable viscosity. These results are plotted in Fig. 7 as the "iterative solution" which agrees with the observed data within the

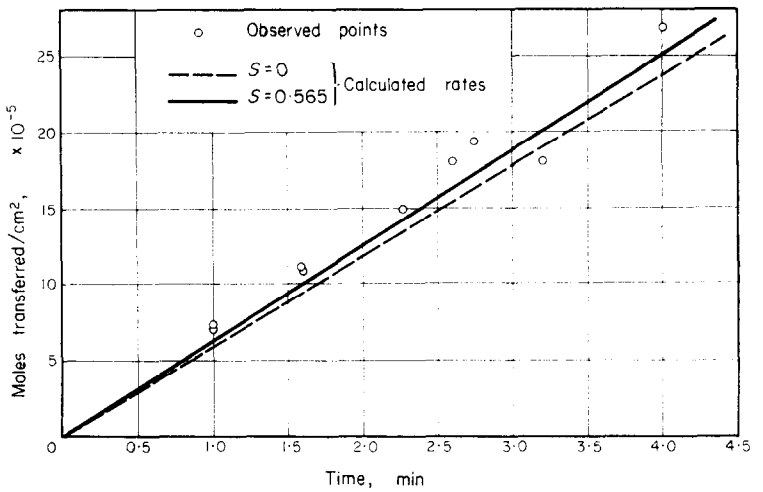

FIG. 5. Mass-transfer measurement for copper sulfate in water 25°C, 67 rev/min. Theoretical ratio from equations (5), (6), and the numerical solution of equation (1) for $S = 0{\cdot}565$ and $S = 0$. Disc diameter = 2 in.

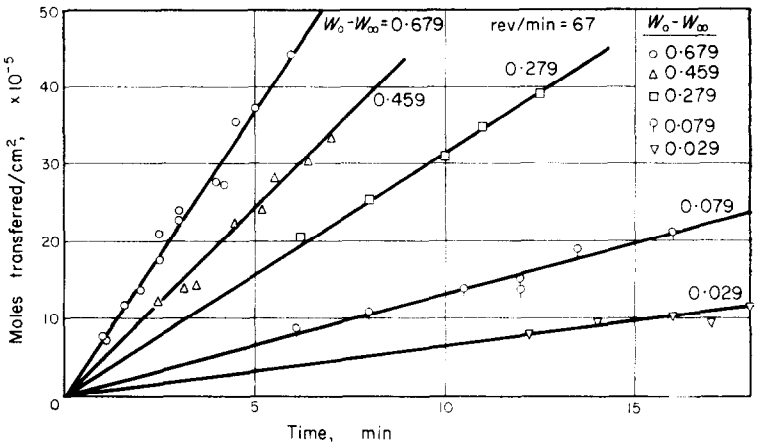

FIG. 6. Mass-transfer measurements for sucrose in water, 25°C, 67 rev/min. Solid line represents best fits to the data. Disc diameter = 2 in.

experimental error. The large error in the experimental Sherwood number ratio is primarily a reflection of the doubtful accuracy of the sucrose–water diffusion coefficients in the concentrated region. The perturbation solution fortuitously predicts the correct Sherwood number ratio at the largest driving force because of cancelling viscosity and interfacial velocity errors.

The effect of concentration level

In the classic film theory, a mass-transfer coefficient is obtained by integrating the relation defining a Fick or Maxwell–Stephen diffusion coefficient across a fictitious stagnant film adjacent to the surface. If the solvent–solute mass flux ratio is S, this approach yields (in terms of mass fractions)

$$\frac{k_w z}{D} = \frac{1}{(1+S)[1-W(1+S)]_{lm}}. \qquad (12)$$

The subscript *lm* denotes a log-mean average, and z is the film thickness. The density and

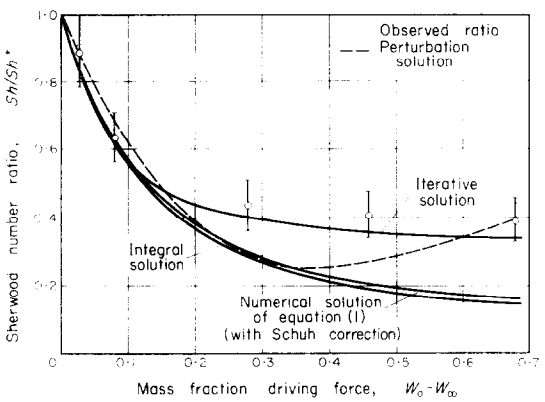

FIG. 7. Sherwood number ratio for sucrose.

diffusivity have been assumed constant. According to equation (12), the effect of changing either W_0 or W_∞ is embodied in the log-mean term.

Writing equation (6) in the same form:

$$\frac{k_w\left[\frac{(\nu_0/\omega)^{1/2}}{-\theta_0'}\right]}{D_0} = \frac{1}{1 - W_0(1 + S)}. \qquad (13)$$

In equation (13), the effect of changing W_0 and W_∞ is more complex than a simple log-mean average. In addition to the right hand side, the magnitude of the driving force affects θ_0' which is a function of the parameter ϵ_V of equation (3). To illustrate the importance of the

$$1 - W_0(1 + S)$$

term in the high driving force transfer experiments described previously, the left-hand side of equation (13) has been plotted as a function of $W_0(1 + S)$ in Fig. 8. k_w was taken from the data (except for sucrose experiments at driving forces greater than 0·1 which were not used) and θ_0' was calculated from the numerical solution to equation (1).† The solid line represents

$$[1 - W_0(1 + S)]^{-1}$$

The variation of the mass-transfer coefficient with this group is a direct reflection of the definition and use of a Maxwell–Stephen rather than a Fick diffusion coefficient in the species

† Although W_∞ does not appear in the parameters of Fig. 8, it is implicit in the solution of equation (1) and has been included in the calculation for each case.

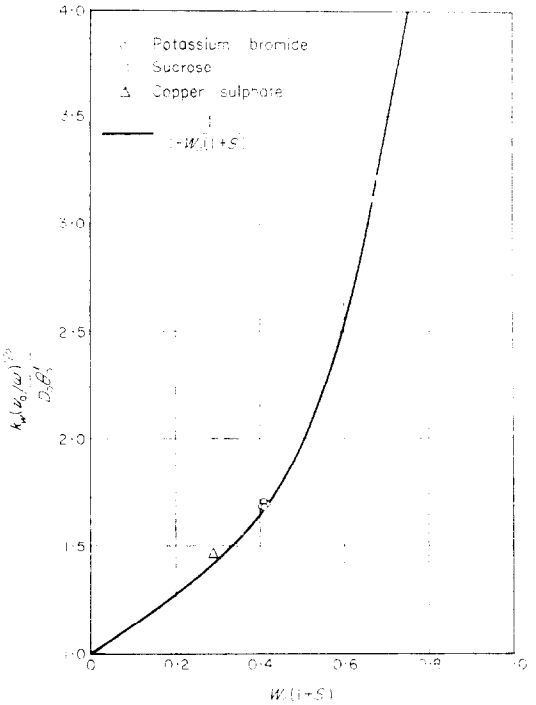

FIG. 8. The effect of surface concentration on the mass-transfer coefficient.

conservation relation. A discussion of the difference between the two can be found in reference 3.

An important practical implication of these results is that a mass-transfer coefficient at one pair of bulk and surface concentrations cannot be corrected for a different driving force by the simple expedient of using the ratio of

$$[1 - W(1 + S)]_{lm},$$

even if all properties are concentration independent. The change in k_w depends upon the ratios of $[1 - W_0(1 + S)]$ and θ_0' at the two concentration levels. Even if the flow is too complicated for analysis, the latter ratio can be estimated from either the perturbation or integral solutions.

ACKNOWLEDGEMENT

This work was carried out under a grant from the National Science Foundation.

REFERENCES

1. W. G. COCHRAN, *Proc. Camb. Phil. Soc.* **30**, 365 (1934).

2. K. MILLSAPS and K. POHLHAUSEN, *J. Aero. Sci.* **19**, 120 (1952).
3. D. R. OLANDER, *Int. J. Heat Mass Transfer* **5**, 765 (1962).
4. E. M. SPARROW and J. L. GREGG, *Trans. ASME, J. Heat Trans.* (a) **C81**, 249 (1959, (b) **C82**, 294 (1960).
5. I. R. KRICHEVSKII and U. V. TSECKHANSKAYA, *Zh. Fiz. Khim.* **33**, 413 (1959).
6. F. KRIETH, J. H. TAYLOR and J. P. CHONG, *Trans. ASME, J. Heat Trans.* **C81**, 95 (1959).
7. H. SCHUH, *NACA* Tech. Memo 1275 (1944).
8. A. EMANUEL, PhD thesis in Chemical Engineering, University of California, Berkeley (1962).
9. C. R. WILKE, C. W. TOBIAS and M. EISENBERG, *Chem. Eng. Prog.* **49**, 663 (1953).
10. J. TIMMERMANS, *The Physico-Chemical Constants of Binary Systems in Concentrated Solutions*, Vol. 4. Interscience, New York (1960).
11. R. H. STOKES and R. A. ROBINSON, *Electrolytic Solutions*, 2nd ed. Academic Press, New York (1959).
12. A. EMANUEL and D. R. OLANDER, *J. Chem. & Engng Data* **8**, 31 (1963).
13. G. THOVERT, *Ann. Chim. Phys.* **26**, 366 (1902).
14. L. J. GOSTING and M. S. MORRIS, *J. Amer. Chem. Soc.* **71**, 1999 (1949).

APPENDIX

Approximate integral solution to the diffusion equation

The constant property, zero interfacial velocity diffusion equation is [3]:

$$\theta^{*\prime\prime} + a^* Sc\eta^2 \theta^{*\prime} = 0 \qquad \text{(A-1)}$$

The solution, subject to the same boundary conditions as equation (1) is:

$$\theta^* = 1 - \frac{1}{\Gamma(4/3)} \int_0^\chi e^{-t^3}\, dt \qquad \text{(A-2)}$$

where:

$$\chi = \left(\frac{a^* Sc}{3}\right)^{1/3} \eta \qquad \text{(A-3)}$$

The thickness of the diffusion boundary layer (the value of χ at which $\theta = 0{\cdot}01$) as can be obtained by numerical integration of equation (A-2) as $\sim 1{\cdot}4$, or:

$$\delta^* = 1{\cdot}4 \left(\frac{3}{a^* Sc}\right)^{1/3} \qquad \text{(A-4)}$$

An approximate expression for θ^* can be written in terms of the distance variable η/δ^* as:

$$\theta^* = a_o + a_1 (\eta/\delta^*) + a_2 (\eta/\delta^*)^2 + a_3 (\eta/\delta^*)^3 + a_4 (\eta/\delta^*)^5$$

The five constants are evaluated by the conditions:

$$\theta^*(0) = 1$$
$$\theta^{*\prime\prime}(0) = 0$$
$$\theta^{*\prime\prime\prime}(0) = 0$$
$$\theta^*(1) = 0$$
$$\theta^{*\prime}(1) = 0 \qquad \text{(A-5)}$$

The first and fourth conditions are reflections of the boundary conditions. The second and third conditions can be obtained directly from equation (A-1). The last condition requires that the concentration profile have zero slope at the outer edge of the boundary layer. These conditions yield, up to the fourth power in (η/δ^*):

$$\theta^* = 1 - 4/3\,(\eta/\delta^*) + 1/3\,(\eta/\delta^*)^4 \qquad \text{(A-6)}$$

This expression reproduces the exact profile to within 10 per cent at all positions. In the presence of property variations and an interfacial velocity, equation (A-4) is no longer an adequate representation of the diffusion boundary-layer thickness. It will be assumed, however, that the form of equation (A-6) remains a valid approximation to the concentration profile if δ^* is replaced by the actual boundary-layer thickness, δ, an estimation of which will be presented shortly.

Substituting equation (A-6) (with the superscript * removed) and equation (10) into equation (1) and integrating from $\eta = 0$ to $\eta = \delta$ yields:

$$Sh = -\theta_o' = \frac{2/9\, a Sc_o\, \delta^2}{1 - 0{\cdot}027\,\gamma + \epsilon_V - \epsilon_\rho\,(0{\cdot}856 - 0{\cdot}540\,\gamma - 0{\cdot}388\,\beta)} \qquad \text{(A-7)}$$

For constant property, zero interfacial velocity case, δ^* can be eliminated from equations (A-6) and (A-7), with the result:

$$Sh^* = -\theta_o^{*\prime} = 2/9\, a^* Sc\delta^{*2} = [2/9\, a^* (4/3)^2]^{1/3} Sc^{1/3} = 0{\cdot}59\, Sc^{1/3} \qquad \text{(A-8)}$$

The constant 0·59 in equation (A-8) is 0·62 by the exact solution [see equation (7)].

In order to evaluate δ in the general case, the form of equation (A-4) was retained and the following modifications assumed:

(1) the one third power of the diffusivity is averaged across the boundary layer: $(D^{1/3})_{AVG} = \int_0^1 D^{1/3}\,d\theta$ where $D(\theta)$ is given by equation (10).
(2) The viscosity variation is accounted for by multiplying α^* by the Schuh correction factor [equation (2)]. The kinematic viscosity in the Schmidt number of equation (A-4) retains its wall value, ν_o, since this is used only as a dimensional reference parameter.
(3) Variable density and interfacial velocity are accounted for by multiplying the constant property thickness by a perturbation expansion in ϵ_V and ϵ_ρ.

With these assumptions, the expression for the variable property layer thickness is:

$$\delta = \delta^* (1 - 0{\cdot}222\,\gamma - 0{\cdot}167\,\beta)(1 + 0{\cdot}23\,\epsilon_V - 0{\cdot}10\,\epsilon_\rho)\left(\frac{\rho_o \mu_o}{\rho_\infty \mu_\infty}\right)^{1/6} \quad \text{(A-9)}$$

The coefficients of ϵ_V and ϵ_ρ were determined empirically from numerical solutions of the diffusion equation with several difierent values of ϵ_V and ϵ_ρ (with constant diffusivity).

Substituting equation (A-9) into equation (A-7) and using the binomial theorem to combine like powers of ϵ_V and ϵ_ρ yields an estimate of the Sherwood number. Division by equation (A-8) then results in equation (11).

It was found that powers of ϵ_V and ϵ_ρ, β, and γ higher than the first could be neglected with little loss in accuracy for a broad range of property variations.

Résumé—On a mesuré expérimentalement et comparé avec la théorie l'effet de gradients de concentration élevés sur la vitesse de transfert de masse à partir d'un disque en rotation. On a trouvé que les vitesses mesurées étaient en accord avec les solutions numériques de l'équation de la diffusion avec des propriétés variables et une vitesse interfaciale finie. On a comparé aussi les données avec les solutions intégrale et approchée par la méthode des perturbations de l'équation de la diffusion. Les systèmes examinés étaient l'acide benzoïque, le bromure de potassium, le sucrose et le sulfate de cuivre en solution dans l'eau. Les variations de densité, de visosité et de diffusivité et l'existence d'une vitesse interfaciale produite par la diffusion peuvent donner des différences aussi grandes qu'un facteur multiplicatif de deux entre les nombres de Sherwood actuels et ceux correspondant à des propriétés constantes et une vitesse interfaciale nulle.

Zusammenfassung—Der Einfluss grosser Konzentrationsgradienten auf den Stoffübergang an einer rotierenden Scheibe wurde experimentell ermittelt und mit der Theorie verglichen. Die gemessenen Stoffübergangsraten stimmten überein mit den numerischen Lösungen der Diffusionsgleichung für veränderliche Stoffwerte und endliche Grenzflächengeschwindigkeit. Die Ergebnisse wurden auch mit angenäherten Störungs- und Integrallösungen der Diffusionsgleichung verglichen. Die untersuchten Systeme bestanden aus Benzoesäure, Bromkalium, Rohrzucker und Kupfersulfat in Wasser. Änderungen der Dichte, der Zähigkeit und des Diffusionskoeffizienten wie auch die Existenz einer diffusionsbedingten Grenzflächengeschwindigkeit können zu Unterschieden zwischen der mit konstanten Stoffwerten und der Grenzflächengeschwindigkeit Null errechneten Sherwood-Zahl und der tatsächlich auftretenden Sherwood-Zahl von der Grösse eines Faktors zwei führen.

Аннотация—Экспериментально изучено влияние больших градиентов концентрации на скорость переноса массы от вращающегося диска, и приведено сравнение с теоретическими данными. Найдено, что полученные экспериментальные значения скорости согласуются с численными решениями уравнения диффузии при конечной скорости на поверхности раздела для случая переменных свойств. Результаты также сравнивались с приближенными решениями волновых и интегральных уравнений диффузии. Исследованные системы представляли собой водные растворы бензойной кислоты, бромистого калия, сахарозы и сульфата меди. Изменение плотности, вязкости и коэффициента диффузии, а также существование скорости на границе раздела, вызванной диффузией, может привести к тому, что действительные числа Шервуда отличаются в два раза от чисел *Sh* для постоянных свойств и отсутствия скорости на границе раздела.